WHIRL FLUTTER AND THE DEVELOPMENT OF THE NASA X-57 MAXWELL

Jennifer Heeg[1], Bret K. Stanford[1], Andrew Kreshock[2], Jinwei Shen[3], Christian B. Hoover[3], and Roger Truax[4]

[1]NASA Langley Research Center, Hampton, VA 23681, USA
[2]US Army Combat Capabilities Development Command, Army Research Laboratory, Hampton, VA, 23681, USA
[3]University of Alabama,, Tuscaloosa, Alabama, 35487, USA
[4]NASA Armstrong Flight Research Center,, Edwards, California, 93523, USA

Keywords: X-57 Maxwell, Whirl Flutter, CAMRAD, DYMORE.

Abstract: The X-57 Maxwell is NASA's all-electric demonstration vehicle. The primary demonstration objective of this flight test program is to show a factor of five reduction in energy consumption. The vehicle includes two large wing tip propellers designed to provide propulsion at cruise conditions and twelve leading edge propellers designed to operate at high lift conditions. The first configuration of the vehicle that will be flight tested has the large wing tip propellers relocated to an inboard wing station. A simplified structural dynamic model of the propulsion system has been generated and coupled with a beam model of the vehicle. Whirl flutter analyses have been performed, examining the stability of the isolated propulsion system and coupled to the beam model of the vehicle. Trimmed flight scenarios for the vehicle include straight and level flight and zero power windmilling conditions. The whirl flutter analyses for this configuration indicate that the configuration will be free of whirl flutter within the required flight envelope.

1 INTRODUCTION

Two constant goals in aeronautics development are improved efficiency and decreased cost. A third desired improvement is to operate aircraft in more environmentally friendly ways. The X-57 Maxwell is NASA's all-electric demonstration vehicle, designed to achieve increased efficiency and a "greener" operating scenario through the integration of electric motors with an aircraft designed to take proper advantage of the available benefits. Electric motors promise significant increases in vehicle efficiency as compared to internal combustion engines [1], but realizing those benefits relies on wing structural design [2] to enable higher aspect ratio, smaller wing area and design freedom for motor placement.

The X-57 configuration has large wing tip propulsers and multiple leading edge high-lift propulsion systems. Supporting these systems and keeping the system structurally stable conflicts with the requirements to make the wing thin and light. The structural challenge is to balance the requirements and arrive at a design, which has sufficient safety margins but doesn't compromise the demonstration goals. Among the issues faced by the structural designers are aeroelastic concerns [3, 4], including the potential for whirl flutter.

Whirl flutter is an aeroelastic instability that can affect the design of propeller-driven aircraft and can lead to vehicle catastrophes as happened in the 1960s with the Lockheed Electra [5]. Whirl flutter occurs as propeller/pylon motions and propeller aerodynamic forces couple, becoming unstable and destructive at critical combinations of airspeed, rotor speed, altitude, rotor power and other vehicle operational parameters. The onset flight condition is highly dependent on vehicle variables such as wing and pylon natural frequencies and mode shapes and propeller aerodynamics and inertia, wing aerodynamics and propeller flexibility.

This paper provides an overview of the X-57 and the whirl flutter concerns for the vehicle. Prior publications have focused on the whirl flutter predictions associated with the wing-tip mounted propeller configuration. In the current paper, the focus will be on the first configuration that will be flight tested, where the propulsion systems are located on the inboard sections of the wings.

2 X-57 MAXWELL

The X-57 Maxwell is NASA's flight demonstrator for distributed electric propulsion (DEP) technology. The primary demonstration objective of this flight test program is to show a factor of five reduction in energy consumption, while a secondary goal is to demonstrate takeoff and landing benefits. The energy consumption goal will mainly be accomplished due to electrification, which provides approximately three times improvement in efficiency compared to the same vehicle powered by combustion engines. Further improvements come from utilizing a smaller wing and from mounting the propellers on the wingtips, reducing energy losses associated with wing tip vortices.

Fourteen propellers, driven by electric motors, will power the X-57. The flight vehicle will feature two systems to provide DEP: large wing tip propellers that will operate at the cruise condition and interact with the wing tip vortex; and small high lift propellers along the wing leading edge to accelerate the flow for improved low speed performance.

Risk and cost have been reduced in the X-57 flight test program by modifying an existing aircraft, the Tecnam P2006T [6], rather than developing the entire aircraft. The program has four configurations, each configuration advances complexity of the vehicle modification ("Mod"). Mod I is the unmodified Tecnam aircraft, used to establish baseline performance quantities. The Mod II configuration, shown in Figure 1a, has the propulsion system of the Tecnam replaced with the electric cruise motors. Testing this configuration allows the project to evaluate new critical systems, establish flight safety aspects of the electric power systems and provide performance data for the electric retrofit aircraft. The Mod III configuration, Figure 1b, features a newly designed and constructed wing, with the wing tip cruise motors. Mod III testing will achieve the primary research objective, demonstrating improved cruise efficiency. The high-lift motors will not be operational during testing of the Mod III configuration. The Mod IV configuration, Figure 1c, will operate the high-lift motors and propellers, addressing takeoff and landing performance.

The X-57 has a tip-to-tip wingspan of 35.5 ft, a reference chord length of 2.1 ft and a total wing area of 66.7 ft^2. While the vehicle gross weight of the original Tecnam aircraft has been maintained, approximately 3000 lb, the wing area of the X-57 is approximately $\frac{1}{3}$ of the Tecnam wing area. This reduction in wing area decreases the skin friction drag and moves the nominal cruise condition to a higher lift coefficient condition.

(a) Mod II. **(b) Mod III.** **(c) Mod IV.**

Figure 1: Vehicle configurations of the X-57 project.

The Mod III/IV wing is made principally from composite material, with three continuous spars from wing tip to wing tip. The main spar is located at the maximum thickness of the airfoil and primarily carries the the normal and axial loads. The forward and aft spars were placed and sized in locations to give additional shear and bending resistance, but primarily to form the forward and aft ends of a wing torsional box. The wing skins form the upper and lower portions of the torsional box and are responsible for carrying the torsional loads. Additional details can be found in Reference [2].

Propulsion system definitions are summarized Tables 1 and 2.

The two cruise propulsion systems each have a 3-bladed propeller connected to a rigid hub with variable blade pitch capability. The cruise propeller blades, made of wood with steel inserts, are high aspect ratio, with approximately 55° of twist change over the span of the blade. The cruise system motors will be nominally operated at 115 horsepower at the target cruise condition. The motor rotational speed is variable, from approximately 1700 to 2700 RPM.

The twelve high-lift propulsion systems each have a fixed-pitch 5-bladed propeller that is significantly smaller than those of the cruise propulsion system. The blades, manufactured from injection molded chopped carbon fiber, are designed to fold when they are not in use. A torsional spring holds each blade in its folded configuration until the propeller is rotated and sufficient centrifugal force is generated to overcome the spring force. The high-lift propeller blades are low aspect ratio, highly twisted blades with a single airfoil cross-section, the MH-114. The high-lift motors will have an operational limit of approximately 5500 RPM, and maximum power of approximately 3 horsepower.

Table 1: Cruise Propulsion System.

Property	Value
Variable pitch blades, Variable speed motors	
Number of Blades	3
Diameter	5 ft
Maximum RPM	2700
Nominal Cruise RPM	2250
Power	115 hp

Table 2: High lift Propulsion System.

Property	Value
Fixed pitch folding blades, Variable speed motors	
Number of Blades	5
Diameter	1.9 ft
Minimum Operational RPM	1000
Maximum Operational RPM	5500
Power	3 hp

3 WHIRL FLUTTER CHALLENGES

The objectives of the X-57 aeroelastic analysis effort are to provide design and operational guidance to the vehicle development process; provide clearance analyses and flutter margin assessments for the three configurations; assess sensitivities to vehicle parameters that are not well defined or contain large uncertainties; and reduce these uncertainties by performing and assessing information from ground tests. Each of the three configurations has unique whirl flutter concerns that must be assessed to satisfy these objectives.

Because the Mod III wing was designed from a blank sheet of paper, prior analysis efforts focused on assessing whirl flutter of this configuration, advising the design process throughout development. Early whirl flutter analyses provided vehicle design guidance for the Mod III configuration, utilizing a semi-span model with fixed centerline boundary conditions and coarse structural definition [7]. Analyses using the full-span free-flight model with the current structural definition show no whirl flutter instabilities near the flight test envelope, but parametric analyses and failure scenarios are being used to further examine regions where caution should be used and to develop flight test reversion processes [8]. This prior work showed that changes in wing stiffness, blade stiffness and propeller blade airfoil shape can significantly reduce the whirl flutter onset conditions. However, the design still demonstrates sufficient margin relative to the planned flight test envelope.

The Mod IV configuration details for the high-lift propulsion system structure are still evolving and will be examined in subsequent publications. The Mod IV configuration is expected to have additional whirl flutter considerations due to the folding blades of the high lift system.

The Mod II configuration was developed to be a low-risk configuration for early flight testing of new systems. The motors are mounted inboard on the wings, replacing the internal combustion engines that are standard on the P-2006 Tecnam aircraft. The motors were connected to the wing using truss structures, which will be discussed in more detail.

4 ANALYSIS TOOLS AND MODELS

Two whirl flutter analysis tools are utilized by the X-57 aeroelasticity team: CAMRAD II [9] and Dymore [10] . CAMRAD II is an aeromechanical analysis for rotorcraft that incorporates several tools, including multibody dynamics, nonlinear elements, structural dynamics, and rotorcraft aerodynamics. Dymore is a finite-element-based multibody dynamics code for the comprehensive modeling of nonlinear flexible multibody systems. The detailed results presented in this paper are all generated with CAMRAD II. Prior publications show good agreement between the two codes for the X-57 Mod III configuration [7].

The CAMRAD II models of the Mod II configuration utilize modal representations of the vehicle and motor-mounting truss structures. Propeller aerodynamics are modeled with lifting-line theory coupled with a linear inflow model. The stability of the model is calculated from an eigenanalysis of the system equations, generating values of damping ratio and frequency from the eigenvalues.

The whirl flutter results are generated by performing eigenanalysis on the system equations after the vehicle parameters have been iteratively adjusted to trim the vehicle at a prescribed set of conditions. Figure 2 shows an illustration of the several methods that were employed to trim the

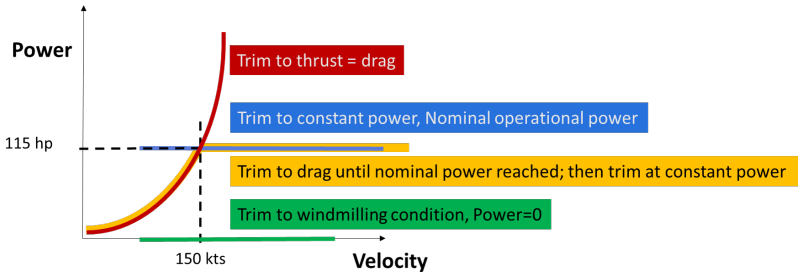

Figure 2: Methods applied to trim the vehicle in CAMRAD II.

aircraft in the whirl flutter analysis. The methods used are as follows. 1) Trimming the aircraft to straight and level flight by setting the thrust to match the vehicle drag. 2) Trimming the aircraft to a specified power level, maintaining all vehicle parameters except the rotor blade angles. This scenario is not a typical flight test scenario, as the vehicle would be climbing and diving. However, this method allows for evaluation of margins relative to flight conditions. A specific example of this type of trimming is when the power is set to zero. This condition is referred to, in this paper, as the windmilling condition. This is important because for many vehicles, windmilling is identified as the most critical whirl flutter condition. 3) A combination of the above, where the power level is increased to increase the vehicle velocity until the maximum power (115 hp) is reached. At higher velocities, the power is then held constant.

Two propeller shaft conditions were modeled and are treated as bracketing the true condition of the shaft as it will act during flight. A "shaft fixed" condition corresponds to a case where the aft end of the shaft is attached to a motor that is infinitely stiff in the shaft rotation degree of freedom. A "free shaft" condition corresponds to a case where the aft end of the shaft is connected to a frictionless bearing. In this scenario, none of the inertia of the rotor system is transferred to the structural dynamic model of the vehicle. These characteristics will be observed in the whirl flutter results to be presented.

5 MOD II: THE FIRST FLIGHT TEST CONFIGURATION

Modifications to the Mod II flight test vehicle were completed in May 2019, including the retrofitting of the cruise motors and propellers, Figure 3. From the perspective of whirl flutter, the Mod II vehicle is different from the Mod III vehicle in the following significant ways. On the Mod II configuration, the propulsion systems are mounted on flexible truss systems connected to the wing at the locations of the original Tecnam aircraft's internal combustion engines. These locations are inboard, rather than at the wingtips. The wing of the Mod II configuration is significantly stiffer than the Mod III configuration, with first wing bending frequencies more than double those of the Mod III vehicle.

5.1 Structure

5.1.1 Vehicle

The Mod II structural dynamics finite element model (FEM) employs classical beam modeling for the different vehicle components, as shown in Figure 4. The vehicle FEM is a modified version of a FEM received from Tecnam, with weights and geometry adjusted to represent the production aircraft, rather than the prototype Tecnam vehicle. It is further modified to remove the mass representations of the fuel and propulsion systems and install the battery mass.

Figure 3: Mod II flight vehicle after modifications.

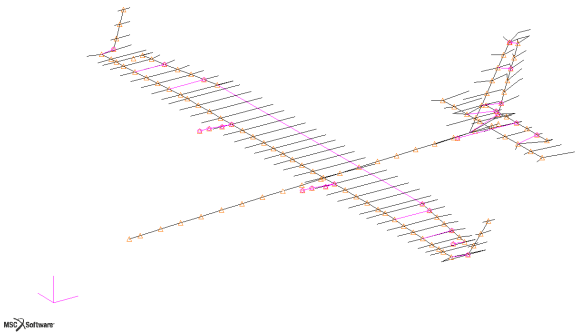

Figure 4: Finite element mode of the Mod II configuration.

The final modification in the current FEM includes of simplified truss structures with masses representing the Mod II motor and motor mount systems, which are described below. The vehicle FEM contains approximately 300 grid points and 700 elements. A list of the mode shapes and natural frequencies for the first twelve vehicle modes are listed in Table 3.

5.1.2 Motor mount: truss structure

A drawing of the truss structure used to mount the new propulsions systems to the wing is shown in Figure 5. A detailed finite element model of the truss structure, shown in Figure 5b, was analyzed to produce mode shapes and frequencies. Based on the modal information from the detailed model, a simplified FEM was generated for connection to the beam representation of the vehicle.

Four truss modes of the detailed FEM are captured in the simplified FEM. These modes are shown in Figure 6: pitch, yaw, fore-aft translation and torsion about the shaft. Frequencies calculated from different versions of the detailed finite element models of the isolated truss including the mass and inertia of the propulsion system are shown in Figure 7a. The frequency plot shows the variation associated with four methods of connecting the motor face plate to concentrated mass elements representing the propulsion system components. The modeling associated with the third set of frequencies in this plot was chosen as the nominal configura-

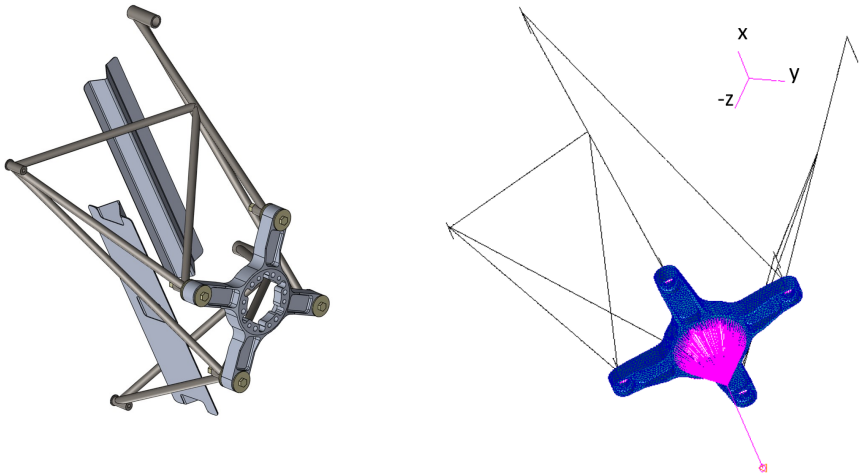

(a) CAD representation. **(b) Detailed finite element model.**

Figure 5: Motor mount structure.

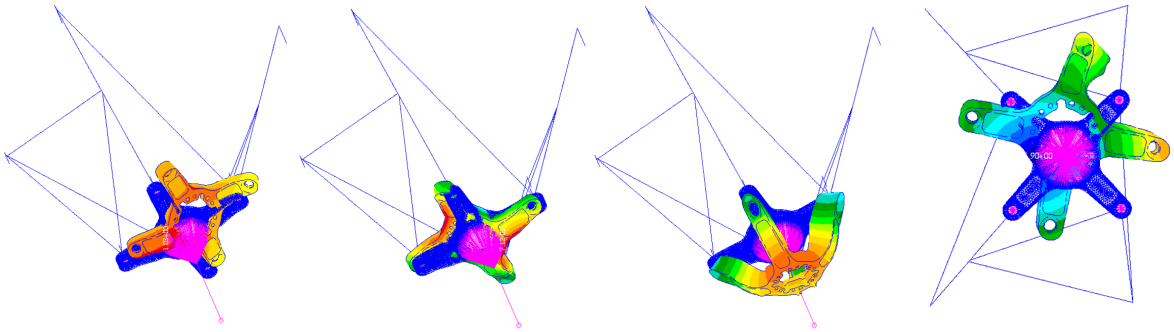

(a) Pitch. **(b) Yaw.** **(c) Fore-aft.** **(d) Torsion.**

Figure 6: Mode shapes of the detailed finite element model of the truss structure.

Table 3: Mode shapes and frequencies from the Mod II FEM.

Modal frequencies, Hz	**Mode shape description**	**Symmetric (S) or Antisymmetric (A)**
0	6 Rigid Body Modes	
7.93	Wing 1st Vertical Bending	S
10.15	Fuselage 1st Lateral Bending + Aft Fuselage Torsion	A
12.95	Wing 1st Vertical Bending + Aft Fuselage Torsion	A
13.00 (17.0)	Stabilator Rotation (GVT-updated value)	S
15.59 (15.2)	Stabilator Rotation + Fuselage 1st Vertical Bending – Out of Phase (GVT-updated value)	S
16.06	Aft Fuselage Torsion + Wing 2nd Vertical Bending– In Phase	A
19.63	Vertical Tail 1st Lateral Bending + Aft Fuselage Torsion	A
19.92	Rudder Rotation	A
23.99	Wing 2nd Vertical Bending + Fuselage 1st Vertical Bending + Stabilator 1st Vertical Bending	S
25.57	Aileron Rotation	A
29.16	Stabilator 1st Vertical Bending with Rotation + Fuselage 2nd Vertical Bending– Out of Phase	A
33.31	Stabilator 1st Vertical Bending with Rotation + Fuselage 2nd Vertical Bending + Wing 1st in-plane Bending	S

tion. The simplified model of the truss structure was constructed with three mass and inertia components, representing the faceplate, the motor controller and the combined assembly of the propeller, hub and spinner. Each mass was located at the center of gravity of the component or components. Rigid elements connect the mass components together and a separate rigid element connects them to four springs. Each of the four springs was tuned to match the stiffness of one of the four preserved modes of the truss detailed finite element model.

The system frequencies of the isolated truss are compared with system frequencies of the vehicle FEM with the simplified truss incorporated, Figure 7. There are two frequencies for each truss mode because there are two propulsion systems, one on each side of the vehicle. The most significant difference that is produced when the models are combined appears in the pitch mode frequencies. Combining the truss flexibility with the wing flexibility causes the modes to combine. Thus, the pitching motion of the truss structure is distributed among several modes that also include high frequency wing twist modes. It will be shown in the results that this combining makes the motor modes difficult to identify and track. It is important to note that the frequencies of the primary vehicle modes are all lower than the modal frequencies of the truss structure. There are no vehicle flutter mechanisms predicted for the Mod II vehicle with frequencies that lie in the range of the motor truss frequencies.

5.2 Blade aerodynamics

Aerodynamic information for the propeller blades is generated externally to CAMRAD II, and input into the code in a set of tables, known as C81 tables. The required tabular information—sectional lift coefficient, drag coefficient and pitching moment coefficient— is input for a user-defined set of blade span stations, organized as functions of Mach number and angle of attack. ARC2D, a 2-dimensional Navier-Stokes flow solver, was used to generate the airfoil section data at 11 blade span stations. Example blade aerodynamic data sets are shown in Figures 8 and 9 for airfoil sections at 58% and 100% blade span, respectively.

6 RESULTS

6.1 Governor sweeps

Performing trim analyses at a series of prescribed conditions generates solutions where the pitch angle governor modifies the angle of the propeller blade root. Some of the specified conditions in a progressive trim analysis may not have solutions where the power available from the system can match the requested power or the thrust can match the prescribed drag. Trimmed vehicle solutions may not be possible using the aerodynamic information provided for the propellers, because the system cannot generate 0 power at 0 kts airspeed due to blade drag. These untrimmable conditions can be identified by conducting sweeps of the commanded governor angle. Governor sweeps were performed at an altitude of 8000 ft MSL for constant RPM and velocity values. The range of RPM values examined was from 1000 to 2700 RPM; the range of velocity values covered was from 10 and 700 kts (KIAS). Example results showing the power and drag for the cases run at 2250 RPM are shown in Figures 10 and 11. In the figures, each line corresponds to a different flight speed at the nominal RPM specified for cruising flight.

Figure 10a shows the horsepower generated by each motor as a function of the blade angle commanded by the pitch governor for the specified flight velocities. The motor limit, discussed earlier, is 115 hp. Combinations of blade angle and flight velocity that require greater than 115

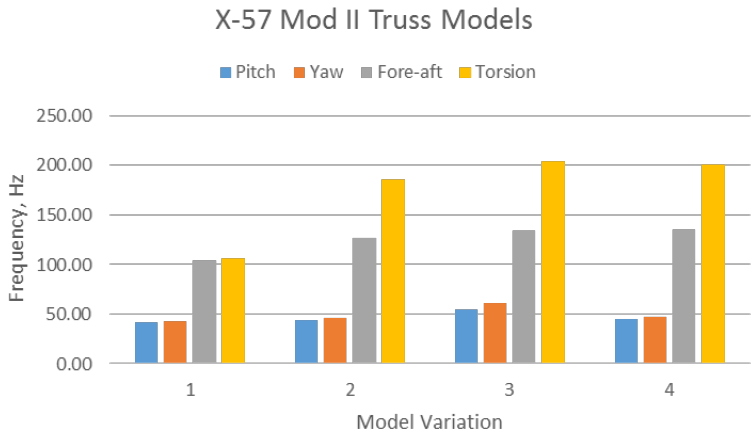

(a) Frequency variations to be used in parametric studies.

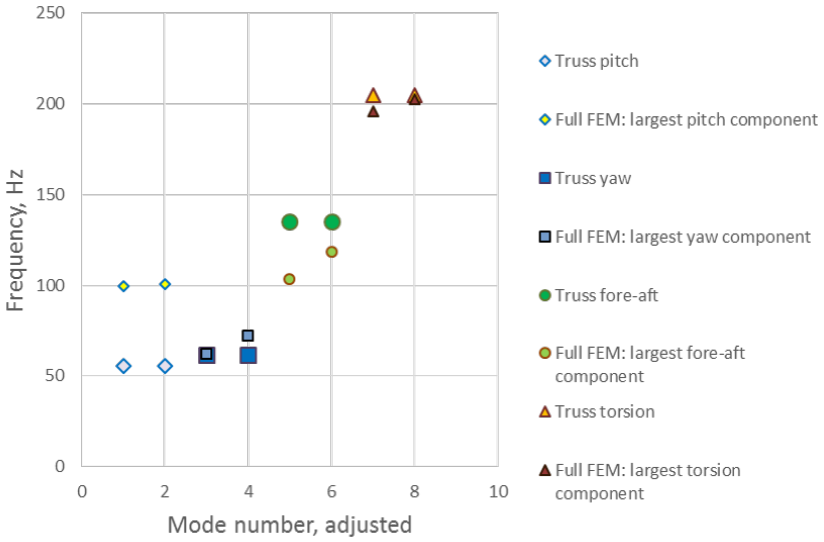

(b) Nominal truss modes, including incorporation into vehicle FEM.

Figure 7: Mod II Propulsion system structural dynamic frequencies.

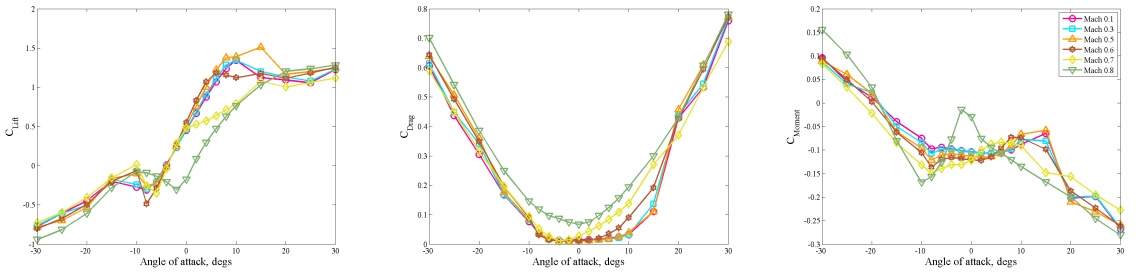

(a) Lift coefficient **(b) Drag coefficient** **(c) Pitching moment coefficient**

Figure 8: Blade aerodynamic data for the cruise propeller, Airfoil section 6 (58% blade span).

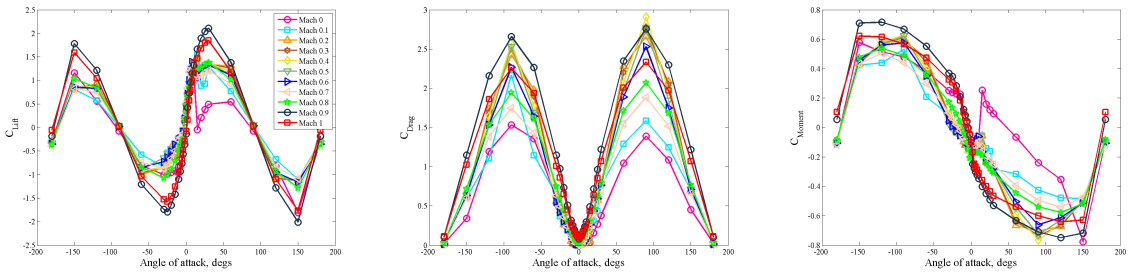

(a) Lift coefficient **(b) Drag coefficient** **(c) Pitching moment coefficient**

Figure 9: Blade aerodynamic data for the cruise propeller, Airfoil section 11 (100% blade span).

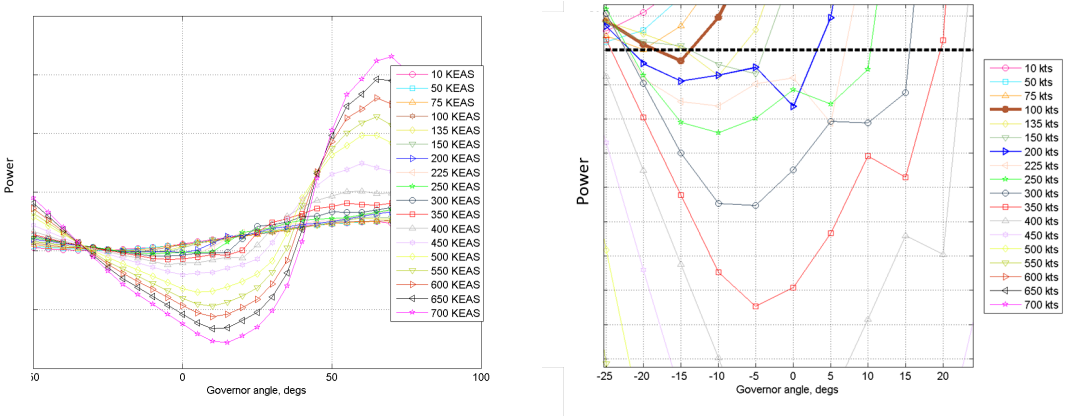

(a) Power. **(b) Enlarged view of transition region for unachievable conditions.**

Figure 10: Power produced by pitch governor sweeps, 2250 RPM.

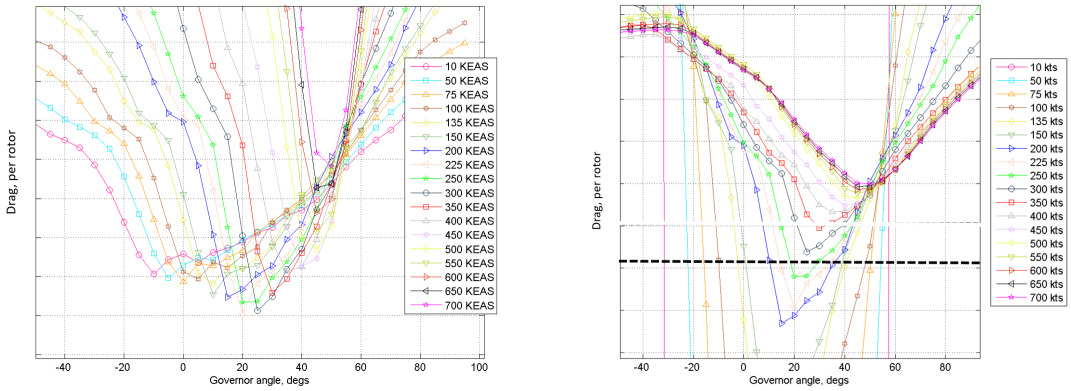

(a) Drag. **(b) Drag per dynamic pressure, enlarged view of conditions near trim.**

Figure 11: Drag produced by pitch governor sweeps, 2250 RPM.

hp are not physically possible for this vehicle. The zero power line indicates the conditions under which windmilling of the system would be achieved at different airspeeds. Because windmilling is considered as the most critical case for this configuration, it is important to notice that there is no governor angle that will achieve zero power for cases below 100 kts at the nominal cruise RPM, 2250. That is, at the cruise RPM, windmilling will not be encountered below 100 kts. Although not presented in this paper, windmilling does occur for lower RPM values for lower airspeeds. This shows that higher RPM operation requires more power for a given blade pitch angle.

Another point to note in examining the results in Figure 10 is that for velocities greater than 200 kts, there are two trim solutions that are possible, one with a negative blade angle and one with a positive blade angle. This feature can cause the trim solution to become erratic if the convergence criteria of the trimming process are not properly controlled. Also, as the RPM decreases, the trim angles for any specified condition grow further apart. There is a minimum power blade angle for all cases. At higher RPM values, this minimum power angle occurs at a larger magnitude negative blade angle, showing that positive blade angles generate more power for a given RPM.

Figure 11a shows the thrust for each rotor, where negative values indicate that the system is generating forward propulsive force. At the cruise condition, 150 kts at 8000 ft MSL, the vehicle drag is approximately 230 lb. To trim the vehicle, each of the two cruise propulsion systems must produce 115 lbs of thrust. Because the drag varies for each flight condition, it is convenient to normalize the drag by the dynamic pressure, as shown in Figure 11b. The vehicle drag per dynamic pressure is 1.92 ft^2, indicated by the horizontal dashed line. Note that the plot has been enlarged to better show this region of the data. The plotted data shows that the line of data generated at 300 kts does not cross the dashed horizontal line, indicating that at 300 kts, the propulsion system— operating at 2250 RPM and beyond— lacks sufficient thrust to overcome the vehicle drag. This indicates another analysis region where a trim solution is not feasible.

6.2 Baseline configuration whirl flutter results

The stability results for the isolated truss structure, trimmed to zero power (windmilling) are examined first. Stability analysis results using the isolated baseline truss structure are presented as critical damping ratio vs velocity in Figure 12. In the figure, each of the truss modes are identified. Only the torsional mode indicates a trend toward instability, which occurs only over the velocity range from 280 kts to 460 kts, well above the vehicle flight envelope. The trend reverses above 460 kts, where stability of the system is shown to increase again. Note that the blade tip Mach number reaches the sonic condition (Mach number = 1.0) at approximately 400 kts.

Identical whirl flutter stability analyses have been performed using the model of the isolated propulsion system and the model with coupled vehicle and propulsion system. The results presented were all trimmed to a windmilling state. Stability results are presented on a root locus plot in Figure 13, where the stable region is the left half plane. The root locus plot shows the migration of the system eigenvalues as the flight condition is increased. In the case of the whirl flutter results presented here, the forward velocity increases, while the rotor speed is held constant at the nominal cruise condition, 2250 RPM. There are four sets of results shown in the root loci. Results with the shaft free and shaft fixed are shown in the plot, using both the full FEM and the isolated mount FEM. An enlarged region of the root locus, focusing on the pitch

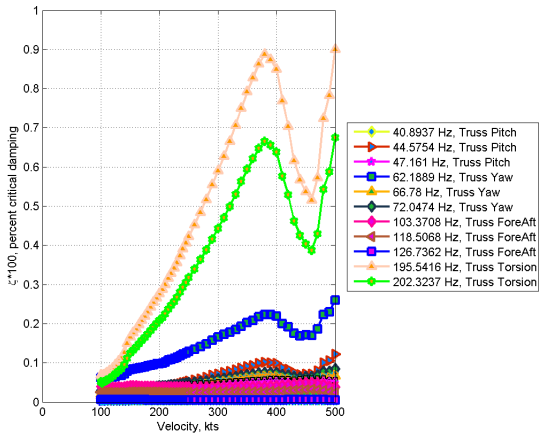

Figure 12: Whirl flutter stability assessment of the baseline isolated truss structure results, damping.

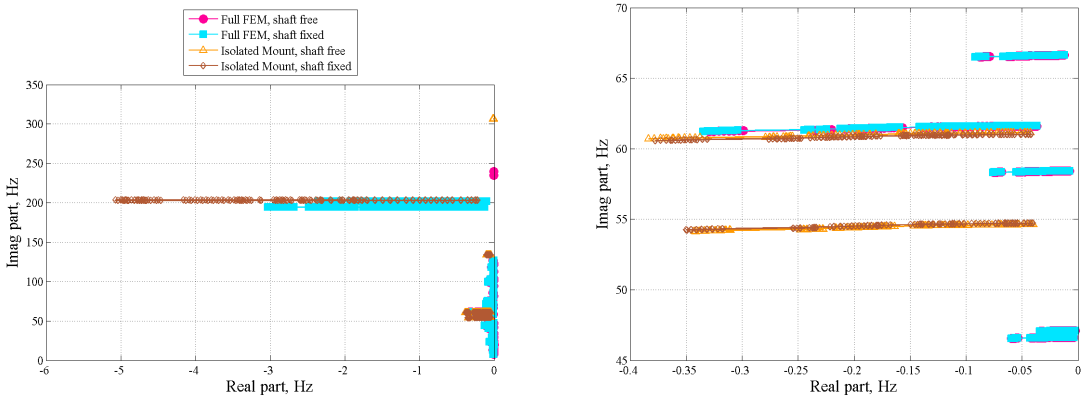

(a) Root locus as velocity is varied. **(b) Enlarged plot to examine pitch and yaw modes.**

Figure 13: Root locus of Mod II vehicle with baseline truss stiffness values, solutions trimmed to windmilling conditions.

and yaw modes is shown in Figure 13b.

All of the cases are shown to be free of whirl flutter. The free shaft cases show the torsional modes of the truss structure at higher frequencies than the fixed shaft cases, as discussed previously. Also, the free shaft cases indicate that the torsional mode frequency of the truss structure does not change significantly with airspeed. This is seen in the figure by the relatively stationary orange and raspberry symbols near 305 Hz for the isolated motor system and 240 Hz for the full FEM. On the other hand, the torsional modes are the most active for the fixed shaft cases, shown by the brown and cyan symbols that migrate to the left.

Critical damping ratio values, calculated from the eigenvalues, for the shaft fixed cases are compared in Figure 14. These results show that the modes and trends with velocity are generally captured by the simplified model.

6.3 Parametric variations and failed component analyses

Parametric variations and analyses that represent failed structural components of the motor mount truss structure were performed. Results for the Mod II configuration are very similar to those generated for the Mod III configuration in Reference [11]. A set of example results for

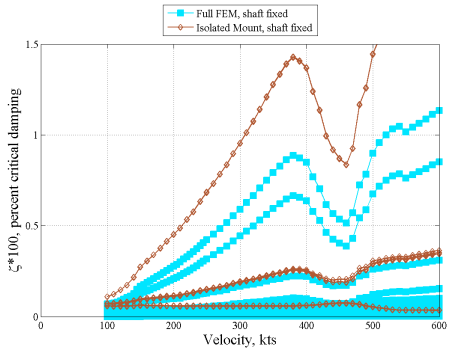

Figure 14: Comparison of damping for full FEM and isolated truss FEM; Shaft fixed cases.

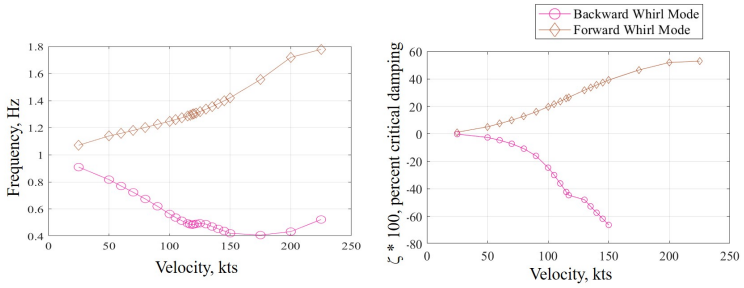

Figure 15: Frequency and damping variation of whirl modes as velocity is varied for system trimmed to windmilling conditions - pitch and yaw modal frequencies reduced to 1 Hz.

the Mod II configuration is shown in Figure 15, where the structural dynamic model has been adjusted so that the pitch and yaw modes of the truss system are equal and have a frequency of 1 Hz. This is an extreme variation from the nominal frequencies, which are between 55 and 65 Hz. Significant destiffening of the truss structure, representing significant structural failures, are required to destabilize the Mod II system.

The results presented show both a backward whirl mode and a forward whirl flutter mode, as predicted by classical techniques and as demonstrated for the Mod III configuration in [12]. Unlike in most types of vehicle flutter, the modes associated with these whirl flutter phenomena don't necessarily manifest by the frequencies coming together. Rather, they are often viewed as single precession degrees of freedom with distinct frequencies.

7 CONCLUDING REMARKS

The challenges associated with whirl flutter for the X-57 have been addressed using multiple analysis tools throughout the project's history. As the project progresses toward flight test, the aeroelasticity team continues to update structural models and geometries as they become available. In the CAMRAD II analyses presented in this paper, the Mod II configuration shows little if any tendency toward whirl flutter. The flight vehicle will be monitored for whirl flutter during a build up approach in flight testing. Each nacelle has been instrumented so that the pitch and yaw behavior can be observed and tracked. As with the full vehicle FEM, it is thought that the vehicle modes may complicate modal identification and tracking. The Mod II flight test, with the isolated motor mount systems for the cruise propulsion systems will partially alleviate this consideration and allow the flight test team valuable experience in assessing whirl flutter in real time.

8 REFERENCES

[1] Moore, M., Goodrich, K., Viken, J., et al. (2013). High speed mobility through on-demand aviation. AIAA Paper 2013-4373. Aviation Technology, Integration and Operations Conference, Los Angeles, CA, August 2013.

[2] Moore, J. B. and Cutright, S. (2017). Structural design exploration of an electric powered multi-propulsor wing configuration. AIAA Paper 2017-0203. AIAA SciTech Forum, 58th AIAA/ASCE/AHS/Structures, Structural Dynamics and Materials Conference, January 9-13, 2017, Grapevine, Texas.

[3] Massey, S. J., Wieseman, C. D., Stanford, B. K., et al. (2017). Aeroelastic analysis of a distributed electric propulsion wing. AIAA Paper 2017-0413. AIAA SciTech Forum, 58th AIAA/ASCE/AHS/Structures, Structural Dynamics and Materials Conference, January 9-13, 2017, Grapevine, Texas.

[4] Heeg, J., Stanford, B. K., Wieseman, C. D., et al. (2018). Status report on aeroelasticity in the vehicle development for the x-57 maxwell. AIAA Paper 2018-3487. AIAA Aviaton Forum, AIAA Applied Aerodynamics Conference, June 25-29, 2018, Atlanta, GA.

[5] Abbott, T., Frank, Kelly, H. N., and Hampton, K. D. (1960). Investigation of 1/8-size dynamic aeroelastic model of the lockheed electra airplane in the langley transonic dynamics tunnel. NASA TM SX 456.

[6] Bergqvist, P. (2011). Tecnam p2006t: Tecnam's entry-level twin has the opportunity to move well beyond the flight school market. *Flying*. "https://www.flyingmag.com/aircraft/pistons/tecnam-p2006t".

[7] Hoover, C. B., Shen, J., Kreshock, A. R., et al. (2017). Whirl flutter stability and its influence ont he design of the distributed electric propeller aircraft x57. AIAA Paper 2017-3785. AIAA Aviation Forum, 58th AIAA/ASCE/AHS/Structures, Structural Dynamics and Materials Conference, January 9-13, 2017, Grapevine, Texas.

[8] Hoover, C. B. and Shen, J. (2019). Whirl flutter analysis of a free-flyng electric-driven propeller aircraft. *Journal of Aircraft*, 56(2). doi:10.2514/1.C035263.

[9] Johnson, W. (1994). Technology drives in the development of camrad ii. In *American Helicopter Society Aeromechanics Specialist Meeting*. San Francisco, CA: American Helicopter Society.

[10] Bauchau, O. A., Bottasso, C. L., and Nikishkov, Y. G. (2001). Modeling rotorcraft dynamics with finite element multibody procedures. *Mathematical and Computer Modeling*, 33(10-11), 1113–1137. doi:10.1016/S0895-7177(00)00303-4.

[11] Hoover, C. B. and Shen, J. (2018). Parametric study of whirl flutter stability of the NASA X-57 aircraft. AIAA Paper 2018-0276. AIAA SciTech Forum, 2018 AIAA Aerospace Sciences Meeting, January 8-12, 2018, Kissimmee, Florida.

[12] Hoover, C. B. and Shen, J. (2019). Fundamental understanding of propeller whirl flutter withmultibody dynamics analysis. AIAA Paper 2019-1864. AIAA SciTech 2019 Forum.